Liu, W., Wen, J., Lin, C.-H., Liu, J., Long, Z., and Chen, Q. 2013. "Evaluation of various categories of turbulence models for predicting air distribution in an airliner cabin," *Building and Environment, 65, 118-131.*

Evaluation of Various Categories of Turbulence Models for Predicting Air Distribution in an Airliner Cabin

Wei Liu[1,3], Jizhou Wen[1], Chao-Hsin Lin[2], Junjie Liu[1], Zhengwei Long[1,*], Qingyan Chen[1,3]

[1]School of Environmental Science and Engineering, Tianjin University, Tianjin 300072, China
[2]Environmental Control Systems, Boeing Commercial Airplanes, Everett, WA 98203, USA
[3]School of Mechanical Engineering, Purdue University, West Lafayette, IN 47907, USA

[*]Corresponding author

Email: longzw@tju.edu.cn
Address: School of Environmental Science and Engineering, Tianjin University, Tianjin 300072, China
Phone: +86-22-2740 9500

Abstract

Flow fields in commercial airliner cabins are crucial for creating a thermally comfortable and healthy cabin environment. The study of flow fields in cabins could be achieved by numerically solving Navier-Stokes equations with a suitable turbulence model. This investigation evaluated three turbulence models in different categories: the RNG k-ε model, LES, and DES for the steady-state flow in the first-class cabin of a functional MD-82 commercial airliner. The measured flow fields under unoccupied and fully-occupied conditions in the first-class cabin were used for validating the turbulence models. The flow in the unoccupied cabin was isothermally forced convection created by air jets from the diffusers, while the flow in the fully-occupied cabin was mixed convection driven by both the jets and thermal plumes from the thermal manikins used to simulate passengers. This study found that the RNG k-ε model gave acceptable accuracy in predicting the airflow in the unoccupied cabin where the flow was simple, but not for the complicated flow in the fully-occupied cabin. The DES gave acceptable flow fields for both cabins. The LES performed the best and the results agreed well with the experimental data. Comparing the measured flow fields in the two cabin conditions, this study found that the thermal plumes from the heated manikins had a significant influence on the flow fields, but little influence on the turbulence.

Keywords: Airliner cabin; Flow field; Turbulence model; CFD simulation; Validation

1. Introduction

Nowadays, more and more people are traveling by air, and the flying public is becoming more concerned about the cabin environment. Since the cabin environment could be too hot or too cold and air contaminants such as ozone, carbon monoxide, various organic chemicals, and biological agents could exist in cabins [1], the cabin environment needs further improvement. In commercial airliner cabins, the air distribution is used to regulate the air temperature and air

velocity to create a thermally comfortable environment and to provide adequate ventilation to reduce gaseous and particulate contaminants for maintaining a safe and healthy environment. Therefore, to improve the cabin environment, the air distribution should be carefully studied.

To study the air distribution in an airliner cabin, Computational Fluid Dynamics (CFD) simulations have become a practical approach. Since Nielsen [2], who was the first one to apply CFD to room airflow prediction, applications of CFD for airflow predictions in enclosed spaces have become popular [3]. Compared with experimental study, CFD simulation is less expensive and more efficient. However, since the turbulence models in CFD used approximations, the simulation results may contain uncertainties. Therefore, the CFD results need to be validated by corresponding experimental data before CFD can be used for further studies.

We reviewed CFD application for airliner cabins [4] and found that the CFD models mainly used were Reynolds Averaged Navier-Stokes equation (RANS) models and Large Eddy Simulation (LES) [5, 6]. For example, Lin et al. [7] studied airflow in a section of a twin-aisle aircraft cabin with the Re-Normalization Group (RNG) k-ε model [8]. The simulation substantially under-predicted the turbulence intensity, especially in and around the breathing zone. Zhang et al. [9] also used the RNG k-ε model to study the airflow in a twin-aisle, economy-class section of an airliner cabin. Poor agreement was found between the computed results and the experimental data, and they concluded that the deviation was due to the difficulties in measuring accurate flow boundary conditions from the air supply diffusers. Singh et al. [10] used the RNG k-ε model to simulate the airflow in a cabin mockup without occupants and with occupants. The inlet air velocity in their study was uniform. However, due to the lack of reliable experimental data, their study could not make quantitative comparisons between the simulated results and experimental data. Lin et al. [7] conducted a LES to obtain the turbulent flow in a generic cabin mockup. The turbulence level predicted was in fairly good agreement with the experimental data. However, these studies did not compare the performance on prediction of air flow field of different categories of turbulence models. Moreover, since numerous turbulence models have been developed in the past decades, many of them may be used in predicting airflows and turbulence in enclosed environments. Besides the RANS models and LES, Detached Eddy Simulation (DES) [11] has been widely used to predict airflow in indoor environments. Roy et al. [12] compared DES and RANS and Jouvray et al. [13, 14] compared DES, LES, and RANS and found that DES appeared to be a promising model, giving good agreement on velocity and Reynolds stresses. It is indispensible to evaluate the generality and robustness of the DES for airflow prediction in aircraft cabins.

The studies above included some experimental data for validating the CFD results. Through a more extended literature search, this investigation found that most of the experimental measurements were conducted in cabin mockups with only a few rows of seats or no seats at all [9, 15, 16, 17]. The cabin mockups were different from real aircraft cabins, especially in the air supply system and internal furnishings. The influence of these differences on the airflow is mostly unknown. Mazumdar et al. [18] concluded that the flow and contaminant transport obtained using the small-scale water cabin model may not be the same as in a full-scale aircraft cabin because it is difficult to achieve flow similarity. Therefore, it is necessary to use a real aircraft cabin to obtain reliable and high quality experimental data. Moreover, most of the former experimental studies [19-24] applied optical measuring techniques such as Particle Tracking Velocimetry (PTV), Particle Streak Velocimetry (PSV), and Particle Image Velocimetry (PIV). These optical anemometries could only measure in the spaces where a laser light sheet can penetrate. When they were used in an aircraft cabin, passengers (typically manikins) and seats

would block the laser light sheet, so no airflow could be measured in the lower part of the cabin. Zhang et al. [9] applied Ultrasonic Anemometers (UA), which can provide three-dimensional, point-by-point airflow information, to measure the flow field in a cabin mockup. The measured data had low resolution because the UA sensor was very expensive, so they used only two UAs in their experiment. Our previous paper [25] reported our effort to obtain accurate cabin geometry, boundary conditions of diffusers, and high-resolution flow fields with nine UAs in an unoccupied, first-class cabin of a functional MD-82 commercial airliner. The experimental data in unoccupied conditions could be used to evaluate the turbulence models, but it is not sufficient since the occupied conditions are more important for passengers and crew. Therefore, it is necessary to obtain a high-resolution flow field in occupied condition for validating turbulence models.

Therefore, this study measured further the boundary conditions and flow fields in fully-occupied conditions with heated manikins in the first-class cabin of an MD-82 commercial airliner. The measured data together with that of the unoccupied cabin [25] was used here to compare it with the corresponding numerical simulation results by three turbulence models in different categories: RNG k-ε model, LES, and DES. This effort would be able to identify a suitable model for further studies of airflow in airliner cabins and provide engineers a good sense on the model performance and computing costs.

2. Research Method

The main objective of our study was to evaluate different CFD turbulence models by using high quality flow data measured in a functional MD-82 airliner cabin. Since the experimental data from our previous experiment [25] was insufficient for the validation, additional measurements for the cabin under fully-occupied conditions were conducted. The following describes the method used in the experimental measurements and CFD modeling.

2.1 Experimental measurements

This investigation used the same MD-82 aircraft [25] for additional experimental measurements. Readers may refer to that paper for more detailed information on the measuring technique. The additional measurements were for a fully-occupied, first-class cabin. This investigation built thermal manikins by wrapping them with nickel-chromium wires that were 2 mm in diameter with a resistance of 32 Ω/m. The sitting height of the manikins was 1.28 m and the surface area of the manikins was 1.334 m^2. The manikins were heated by 380 V direct electrical current, and the sensible heat production for each of them was controlled at 75 W. The heat generated for each part of the manikin was also controlled according to the average level of humans [26], as shown in Table 1.

Table 1. Heat distribution of the thermal manikin

Body segments	Heat generated by thermal manikin (W)	Percentage (%)
Head and neck	5.7	7.6
Trunk	20.1	26.8
Left arm	8.2	10.9
Right arm	8.2	10.9

Left leg	16.4	21.9
Right leg	16.4	21.9
Total	75.0	100.0

The supply air temperature from the diffusers to the cabin was controlled at 20±1 ºC. Due to the existence of the manikins, the measuring resolution was decreased to 0.1 m high × 0.2 m wide in a cross section, compared with 0.1 m high x 0.1 m wide in the unoccupied cabin. In addition to the air velocity, this study also measured the temperature field by 64 thermo-couples with the same resolution as that for the flow field. The measurements were conducted in three cross sections and three longitudinal sections (window seats, aisle seats, center of the aisle) in the first-class cabin, as shown in Figure 1. This investigation repeated the measurements at least once to ensure the reliability of the experimental data.

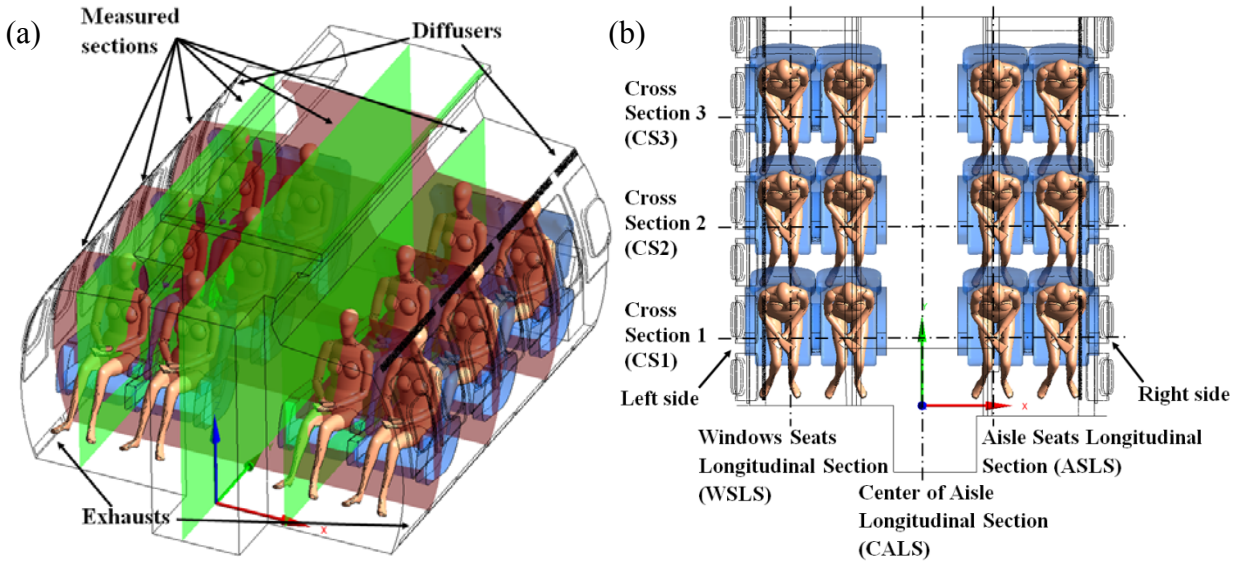

Figure 1. Schematic of the fully-occupied, first-class cabin and measured sections: (a) perspective view and (b) plane view.

2.2 Numerical method

This study tested three different turbulence models: RNG k-ε model, LES, and DES, since these turbulence models are either widely used or proposed mainly for indoor airflow modeling [27]. The governing equations for all three turbulence models can be written in a general form:

$$\rho\frac{\partial\bar{\phi}}{\partial t}+\rho\bar{u}_i\frac{\partial\bar{\phi}}{\partial x_i}-\frac{\partial}{\partial x_i}[\Gamma_{\phi,eff}\frac{\partial\bar{\phi}}{\partial x_i}]=S_\phi \qquad (1)$$

where ϕ represents the flow variables (velocity, enthalpy, and turbulence parameters), $\Gamma_{\phi,eff}$ the effective diffusion coefficient, and S_ϕ the source term. When $\phi=1$, $\Gamma_{\phi,eff}$ and S_ϕ equal zero, and equation (1) becomes the continuity equation. Table 2 presents how the general form can be used to describe the three turbulence models.

For the RNG k-ε model, u_i is the velocity component in *i* direction, *p* the air pressure, T the air temperature, *H* the air enthalpy, *k* the kinetic energy of turbulence, *ε* the dissipation rate of the turbulent kinetic energy, μ_t the eddy viscosity, G_ϕ the turbulence production for ϕ, and S the rate of the strain. For the LES, the over bar represents a filtered variable. The τ_{ij}^S and h_j^S represent the subgrid scale (SGS) stress and heat flux. Since Zhang et al. [27] concluded that SGS models had a very similar performance for an indoor environment, this study used the Smagorinsky-Lilly SGS model [28]. Lilly's model adopted the Boussinesq hypothesis and calculates the coefficient C_s. The DES [11] coupled the LES with the Realizable k-ε model. In the DES approach, the Realizable k-ε model was employed in the near-wall regions, while LES was used in the regions away from the near-wall [29]. The LES region is normally associated with the core turbulent region where large turbulence scales play a dominant role. In this region, the DES recovers the respective SGS models. In the near-wall region, the respective RANS model is recovered. Due to the limited space, this paper did not provide a more detailed description of these models as they are widely available in the literature. There are also some coefficients that are case-specific and they are not introduced here. One could refer to the user manual of the commercial code we used, ANASYS Fluent Version 12.0 [29].

Table 2. Coefficients and source term for governing Equation. (1)

CFD models	ϕ	$\Gamma_{\phi,eff}$	S_ϕ	Constants and coefficients
RNG k-ε model	u_i	$\mu+\mu_t$	$-\partial p/\partial x_i-\rho\beta g_i(H-H_0)/C_p$	$\mu_t=C_\mu\rho k^2/\varepsilon; G_{k=}\mu_t S^2; S\equiv\sqrt{2S_{ij}S_{ij}};$ $G_B=\rho g_i(\mu_t/\sigma_{k,t})\partial\overline{T}/\partial x_i;$ $C_{\varepsilon1}=1.44, C_{\varepsilon2}=1.92, C_\mu=0.09,$ $\sigma_{T,t}=0.9, \sigma_{k,t}=1.0, \sigma_{\varepsilon,t}=1.3$
	T	$\mu/\sigma_T+\mu_t/\sigma_{T,t}$	S_H	
	k	$\mu+\mu_t/\sigma_{k,t}$	$G_k-\rho\varepsilon+G_B$	
	ε	$\mu+\mu_t/\sigma_{\varepsilon,t}$	$C_{\varepsilon1}G_k\varepsilon/k-C_{\varepsilon2}\rho\varepsilon^2/k$	
LES	u_i	μ	$-\partial\overline{p}/\partial x_i-\partial\tau_{ij}^S/\partial x_j$	$\tau_{ij}^S\equiv\overline{u_iu_j}-\overline{u}_i\overline{u}_j; h_j^S\equiv\overline{Tu_j}-\overline{T}\overline{u}_j;$ $\tau_{ij}^S=\mu_t(\partial u_i/\partial x_j+\partial u_i/\partial x_j)+\rho\tau_{kk}^S\delta_{ij};$ $\mu_t=\rho(C_s\Delta)^2\sqrt{2\overline{S}_{ij}\overline{S}_{ij}}$
	T	μ/σ_T	$-\partial h_j^S/\partial x_j$	
DES-Rea	k	$\mu+\mu_t/\sigma_{k,t}$	$G_k-\rho\varepsilon+G_B-Y_M+S_k$	$C_1=\max[0.43,\eta/(\eta+5)]; \eta=Sk/\varepsilon;$ $S=\sqrt{2S_{ij}S_{ij}}; \mu_t=C_\mu\rho k^2/\varepsilon;$ $C_\mu=1/(A_0+A_s kU^*/\varepsilon);$ $G_B=\rho g_i(\mu_t/\sigma_{k,t})\partial\overline{T}/\partial x_i;$ $C_{\varepsilon1}=1.44; C_2=1.9; \sigma_k=1.0; \sigma_\varepsilon=1.2$
	ε	$\mu+\mu_t/\sigma_{\varepsilon,t}$	$\rho C_1 S\varepsilon-\rho C_2\varepsilon^2/(k+\sqrt{v\varepsilon})+$ $C_{\varepsilon1}C_{\varepsilon3}G_B\varepsilon/k+S_\varepsilon$	
DES-Rea: DES switches between the Realizable k-ε model and LES				

Since our previous study [25] measured the velocity at one point for each slot, this study assigned the measured velocity for the inlet slot by slot and the velocity on each slot was assumed to be uniform. Pressure outlet was applied on outlet and the reference pressure was set to be 0. The Boussinesq approximation was adopted to simulate the buoyancy effect, while air density was assumed to be constant that has been a common approach for room airflow simulations.

2.2.1 Numerical schemes

For the RNG k-ε model, this study used the SIMPLE algorithm to couple the pressure and velocity. The PRESTO! scheme was adopted for pressure discretization and the first-order upwind scheme for all the other variables. The second-order scheme was tried and it was found that the calculation could not converge. A converged calculation with low order scheme would be more creditable and accurate than a diverged one with high order scheme. A converged calculation with low order scheme would be more creditable and accurate than a diverged one with high order scheme. Besides, the enhanced wall functions [30-32] were adopted in the simulations with RNG k-ε model since the y+ value was less than 30. For LES and DES, this study calculated the transient flows for 1000 s to reach a statistically stable state, and then for another 500 s to obtain statistically steady-state solutions. The time steps for LES and DES were adjusted to ensure that the number of iterations for each time step was between five and ten [29]. The solutions were considered to be converged when the sum of the normalized residuals for all the cells became less than 10^{-6} for energy and 10^{-3} for all other variables. The normalized residuals were defined as:

$$R^{\phi} = \frac{\sum_{cellsP} \left| \sum_{nb} a_{nb}\phi_{nb} + b - a_P\phi_P \right|}{\sum_{cellsP} \left| a_P\phi_P \right|} \tag{2}$$

where ϕ_P and ϕ_{nb} are the flow variable of the present and neighboring cells, respectively; a_P is the center coefficient; a_{nb} are the influence coefficients of the neighboring cells; and b is the contribution of the constant part of the source term and of the boundary condition. This investigation solved steady-state governing equations for the RNG k-ε model and unsteady-state governing equations for LES and DES.

2.2.2 Grid independence test

This study first conducted a grid independence test. Since there were 1920 air-supply slots in the first-class cabin and the size of each slot was 22mm×3mm, the mesh size at the diffusers should not be larger than 3 mm. Our previous study investigated the influence of the mesh size on the slots [33] and compared the velocity field of conditions with 5 facet cells (mesh size of 3 mm) on each slot and that with 22 facet cells. It was found insignificant differences in the predicted flow fields. Therefore, this study assigned 5 facet cells on each slot with the mesh size of 3 mm. If the cabin air volume used a grid size of 50 mm, a size function should be carefully applied due to the scale difference as shown in Figure 2(a). Besides, the seats and the manikins had a lot of geometric details that would generate high skewness cells unless the geometric model was simplified, as depicted in Figure 2(b). Due to the complex geometry, we can only change the global size to generate different meshes in the grid independence test. For the test used for the unoccupied, first-class cabin [25], the cell numbers used were 6, 8.3, and 13 million, respectively. For the fully-occupied cabin, the cell numbers were 6.4, 8.4, and 13 million cells, respectively.

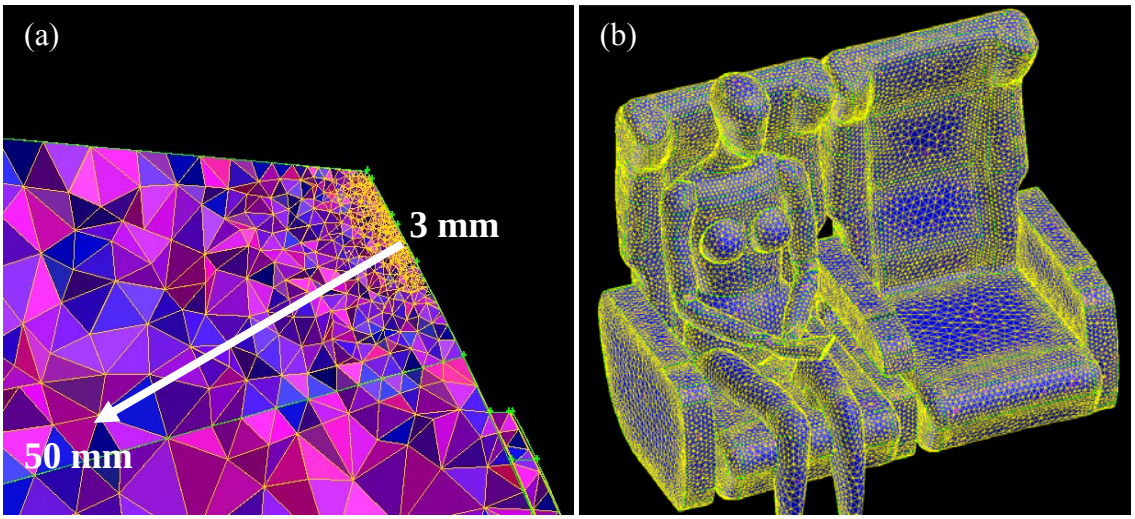

Figure 2. (a) Mesh size at the diffuser region and (b) meshes with size function applied to a manikin and the seats.

Figure 3 depicts the grid independence test with the RNG k-ε model for the unoccupied cabin. At some positions, the velocity profiles with different meshes were similar to those of the experimental data such as Figure 3(a), while large differences were found in Figure 3(b). Figure 3(c) shows partial agreement of the numerical results with the data. It is interesting to note that the calculated results with the finest mesh did not always show a better agreement with the experiment data. The differences among the three meshes were comparable. For the fully-occupied cabin, the grid independence test with the RNG k-ε model also showed that the differences among the three meshes were comparable. Due to the limited space available in this paper, the detailed comparison for the fully-occupied cabin was not shown here. To decrease the computing effort, this study used the mesh with 6 million cells for the unoccupied cabin.

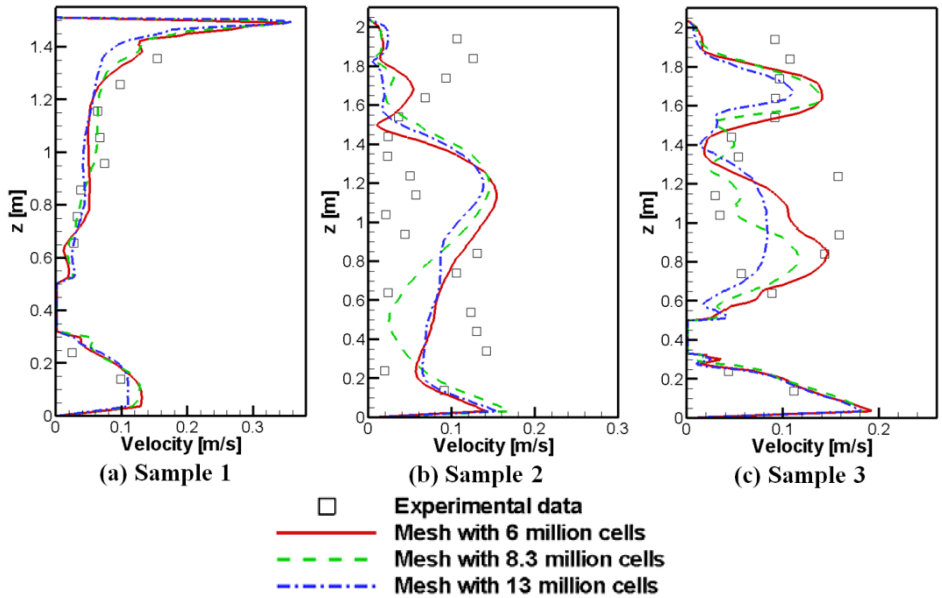

Figure 3. Grid independence test for calculation velocity profiles in the unoccupied cabin with RNG k-ε model

The LES normally requires finer near-wall mesh. The finer the near-wall mesh, the higher accuracy for the simulation with LES. A very fine near-wall mesh distribution for an airliner cabin could require a very large computing capacity. For simplicity, this study used the same mesh distribution for all the three turbulence models.

On the other hand, it is possible that the mesh quality could be poorer in some parts of the cabin when the mesh becomes finer. This investigation used 6, 8.3, and 13 million cells for the grid independent study. The variation was not sufficient large. Ideal variation in grid independent study is to double the grid number in each direction (8 times in total). The variation would require us to test 6, 48, and 384 million cells or 0.2, 1.6 and 13 million cells. This is a dilemma we are facing. If very fine grid (384 million cells) were used, our computer could not handle the grid size. If coarse grid (0.2 million cells) were employed, the cell number would not be sufficient to cover the basic needs for describing the geometry, such as the diffusers. Therefore, for such a complex engineering problem, true grid independent study is very difficult. This study conducted the simulation with a 32-core cluster and it took one month and a half to finish the simulation with LES when the mesh was 6 million cells. With such a powerful cluster, such a long computing time was too long for most engineering applications. This study conducted the simulation with a 32-core cluster and it took one month and a half to finish the simulation with LES and the mesh with 6 million cells. With such a powerful cluster, one month and a half has already exceeded the tolerable computing time in real engineering CFD. The selection of grid number is a trade-off between computer capacity and basic needs for describing geometry. This is very different from conventional grid independent studies. Nevertheless, application engineers should not skip such grid independent study, which still provides a good indication on the grid performance.

3. Results

This study conducted CFD simulations with different turbulence models by using the measured boundary conditions and numerical methods stated in the previous section. The predicted results were then compared with the corresponding experimental data of flow and temperature fields.

3.1 Flow fields in the unoccupied cabin

Figures 4 and 5 compare the predicted flow fields with the measured data at a typical cross section, CS3, and a typical longitudinal section, WSLS, respectively, as shown in Figure 1(b). In the cross section, all three models could predict two large recirculations on each side of the cabin, which agree with the experimental data. The RNG k-ε model predicted a stronger jet from the diffusers on the right side of the cabin. The predicted flow fields by LES and DES were similar and agreed better with the experimental data. However, remarkable differences exist in quantitative comparisons if we look at the two sets of vectors at certain positions. In Figure 4(d), even at the region near the diffusers, the two sets of vectors had some differences in both direction and magnitude. This study measured the fluid boundary conditions with both UAs and hot-sphere anemometers. The measured velocity direction by the UAs may have errors since the probes could not be placed very close to the diffusers. In the longitudinal section, the predicted flow also qualitatively agrees with the experimental data. All three models could predict that the

air under the seats flowed from the back to the front when the air above the seats flowed in the opposite direction.

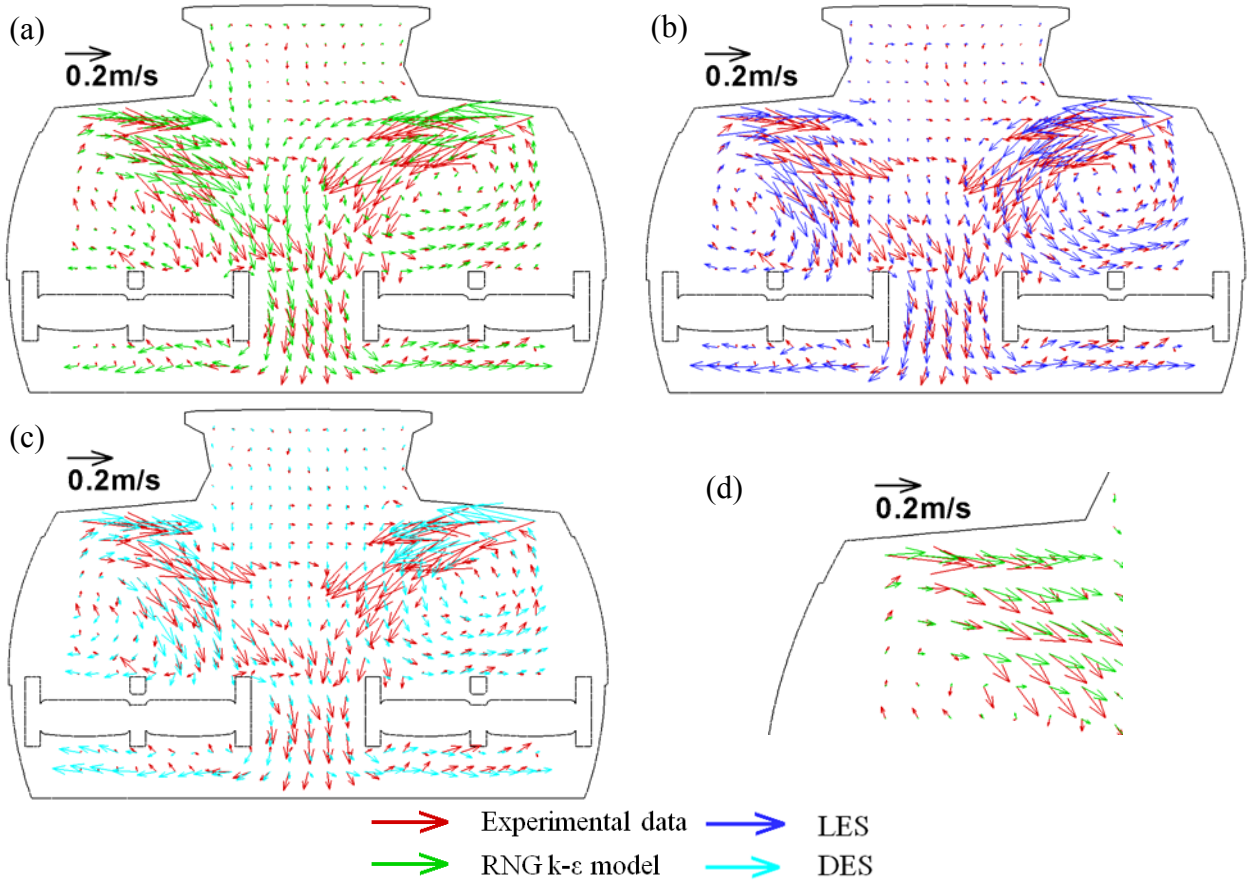

Figure 4. Comparison of the airflow pattern computed and measured at cross section 3 in the unoccupied cabin

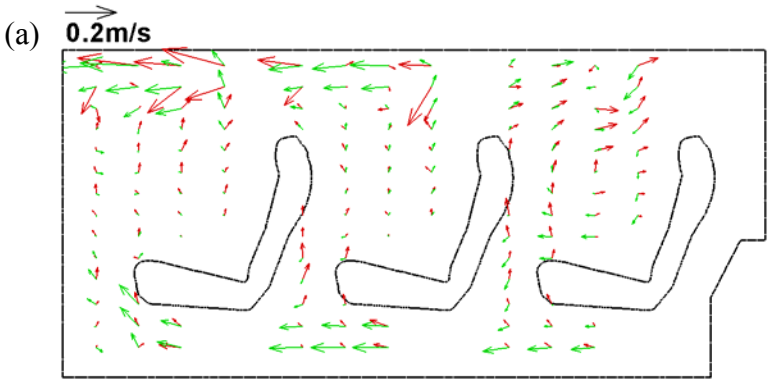

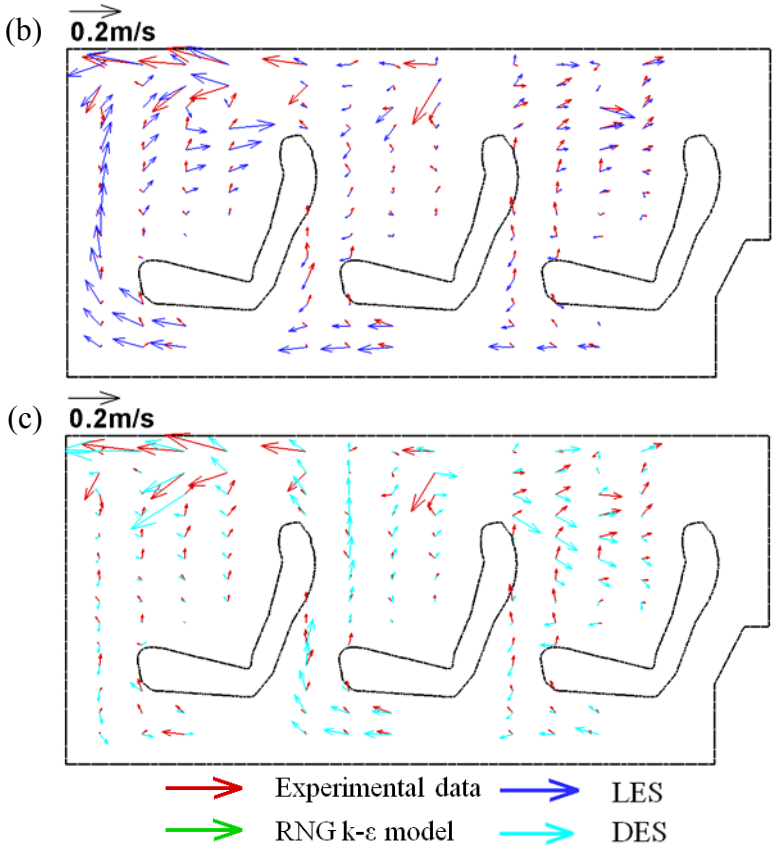

Figure 5. Comparison of the airflow pattern computed and measured at the longitudinal section through the window seats in the unoccupied cabin

This study also compared the predicted flow fields with the measured data at the other sections. Similar results could be found at the other two longitudinal sections. However, at sections CS1 and CS2, the predicted flow fields with all three models differed slightly from the measured results. Even with the LES, as shown in Figure 6, the simulation over-predicted the jet from the right side of the cabin. For the isothermal flow in the unoccupied cabin, the air leakage in the first-class cabin [25] may have had a significant influence on the flow field. Therefore, the differences might have been caused by many different factors, not necessarily the models.

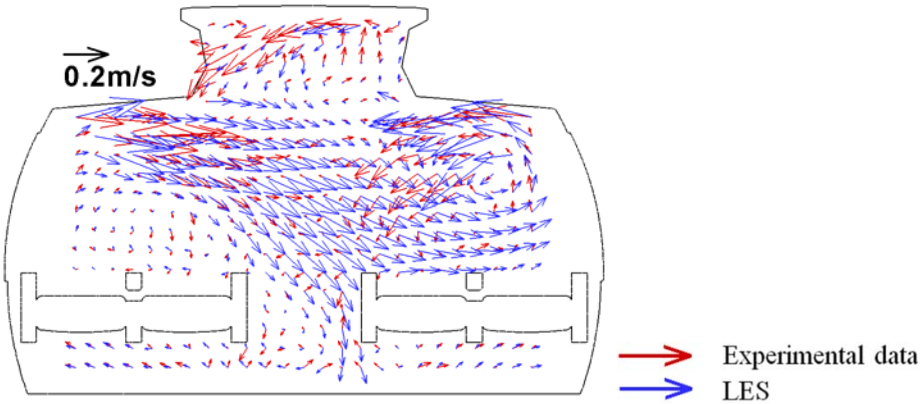

Figure 6. Comparison of the airflow pattern computed by LES with that measured at cross section 1 in the unoccupied cabin

To further analyze the numerical results, Figure 7 compares the velocity profiles at 11 positions at section CS3. The predicted velocity profiles by the RNG k-ε model, LES, and DES were similar at positions 1, 2, 3, 10, and 11, which also agreed well with the experimental data. At those positions located in the center of the cabin, the measured and computed velocity profiles differed significantly. This might have caused the unstable airflow to merge there with the two jets from the diffusers on each side of the cabin. As a whole, the LES and DES could provide slightly better predictions than the RNG k-ε model. However, as the LES and DES used at least 20 times more computing time than the RNG k-ε model, the RNG k-ε model is more preferable for predicting the airflow in an unoccupied cabin.

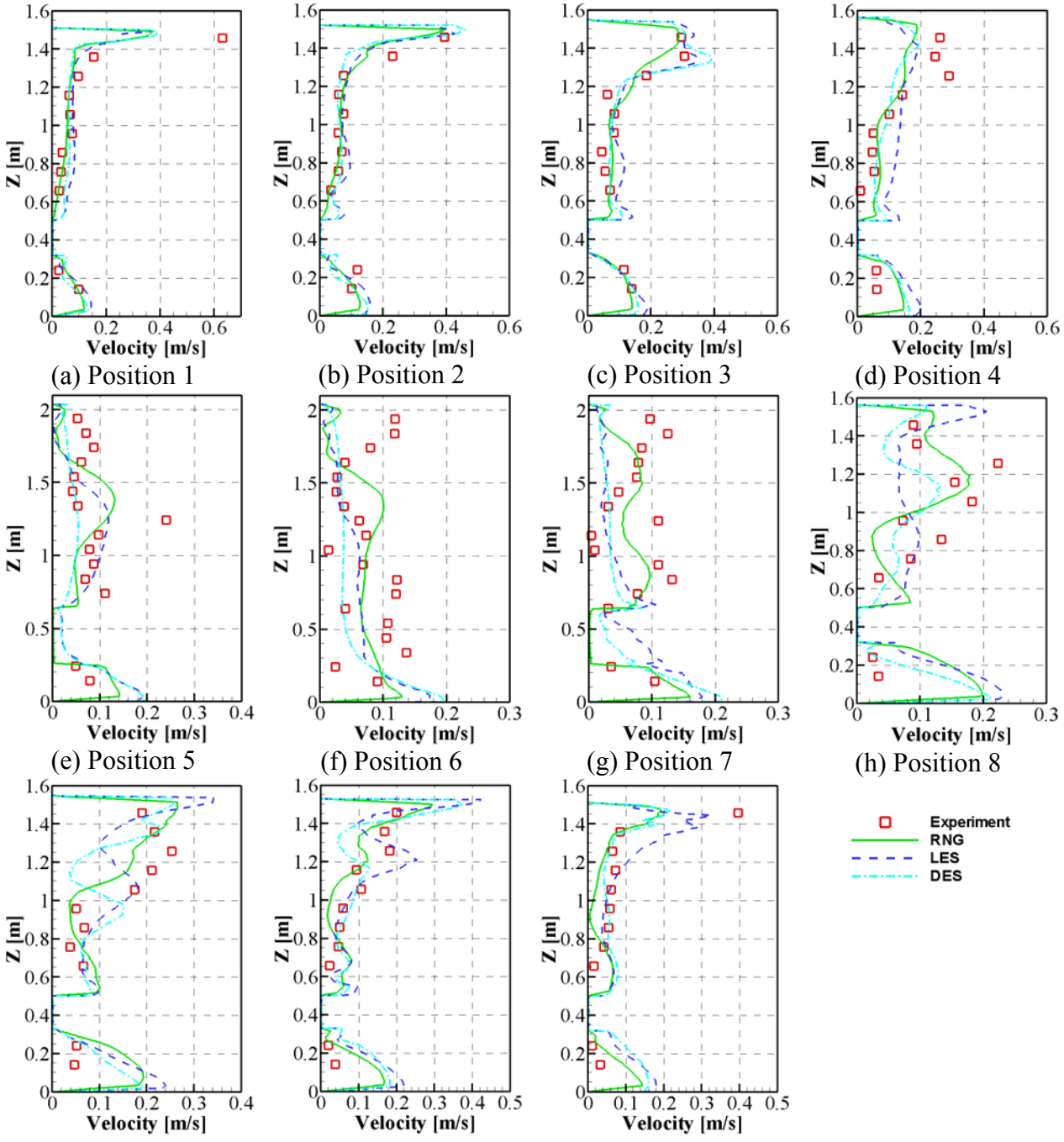

(i) Position 9 (j) Position 10 (k) Position 11

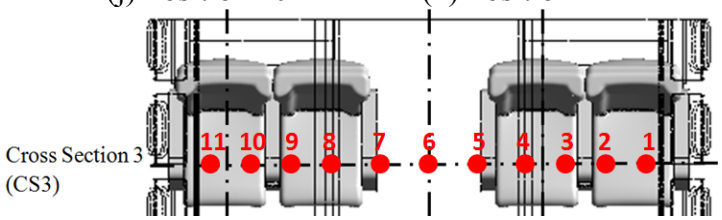

Figure 7. Comparison of the vertical velocity profiles computed and measured at cross section 3 in the unoccupied cabin

3.2 Flow fields in the fully-occupied cabin

For the fully-occupied cabin, Figures 8 and 9 compare the computed and measured flow fields at sections CS3 and ASLS, respectively. In section CS3, the thermal plumes from the heated manikins and the jets from the diffusers counteracted each other, which would diminish the jet momentum. Therefore, the jet from the diffuser had little influence on the manikins, especially the ones in the window seats. Quantitatively, the buoyancy force could be evaluated by the Grashof number (Gr) by specifying the characteristic length as the height of the manikin and the temperature difference between the inlet air temperature and that of the manikin. The inertial force from the jets could be evaluated by the Reynolds number (Re) based on the averaged jet velocity and the characteristic length as distance between the diffuser and the window-manikin's head. The Grashof number was about 3×10^9 and the Reynolds number was about 1×10^5. The relative importance of the two forces can be evaluated by the Richardson number (Ri), which is $Ri = Gr/Re^2 = 0.3 < 1$. Therefore, the forced convection seems more important than the natural convection. In section ASLS, the air under the seats flowed from the front to the back, which was very different from in the unoccupied cabin.

The two figures also compare the performance of the three turbulence models with the data. Figure 8(a) shows that the RNG k-ε model could predict the measured thermal plume on the left side and the flow at the lower central part of the cabin, but it did a poor job on the right side of the cabin. As shown in Figures 8(b) and 8(c), respectively, the LES and DES could predict the thermal plume on both sides of the cabin. However, these two models could not predict the upward flow in the lower central part of the cabin. The jet from the diffuser and the plumes from the manikins made the flow field rather complex. In section ASLS, all three models predicted opposite airflow direction under the seats. For the region above the seats, the predicted flow distributions qualitatively agreed with the experimental data. This study also compared the predicted flow fields with the measured data at the other sections, and similar results could be found except at the section CALS. The inertial flows from the jets and the thermal plumes from the heated manikins in the fully-occupied cabin made the airflow at the center of the cabin very complex. However, the velocity magnitude was small (less than 0.1 m/s at most positions), so the differences may not be very important.

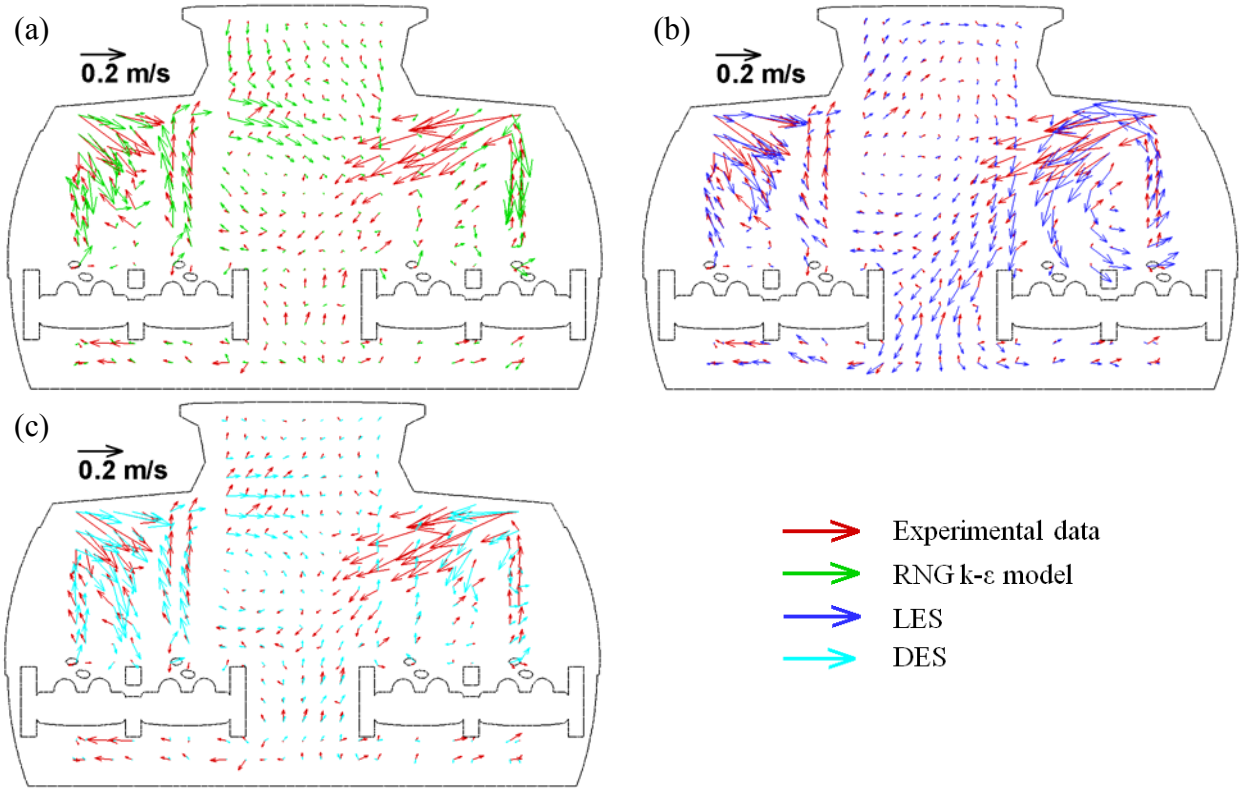

Figure 8. Comparison of the airflow pattern computed and measured in cross section 3 in the fully-occupied cabin

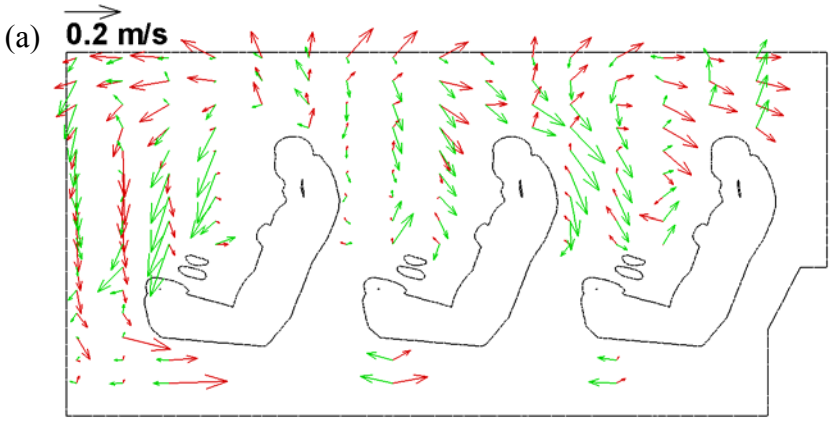

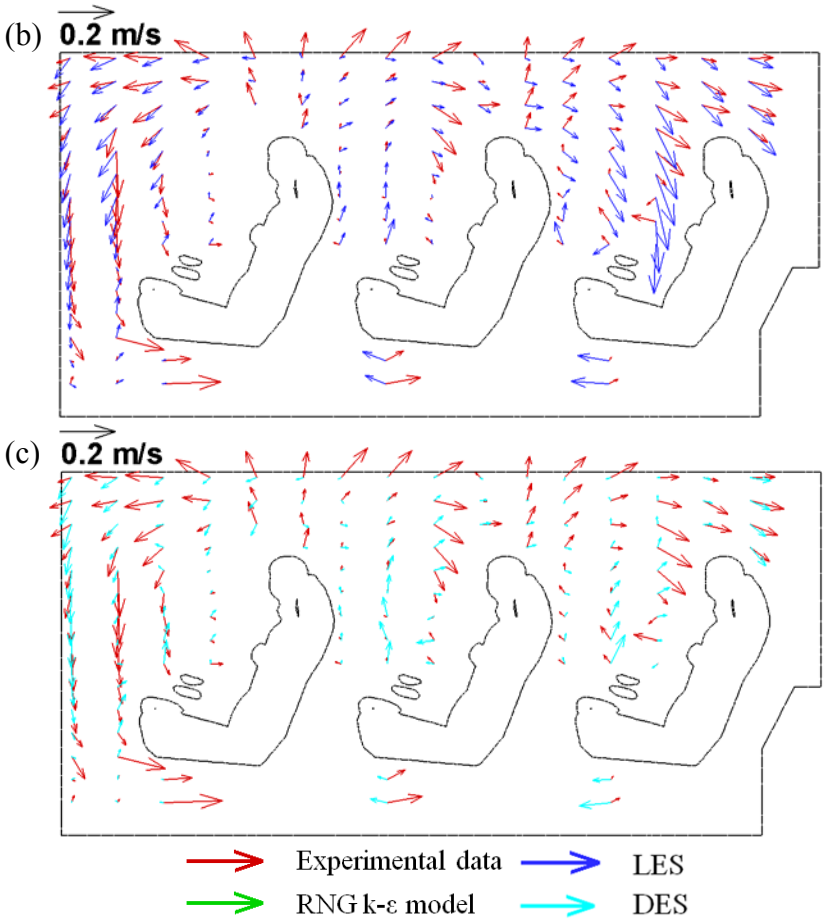

Figure 9. Comparison of the airflow pattern computed and measured in the longitudinal section through the aisle seats in the fully-occupied cabin

This investigation again compares the vertical velocity profiles at the 11 positions at section CS3 in Figure 10. The LES results agree the best with the experimental data, especially at positions 2, 8, and 11. The RNG k-ε model, which over-predicted the velocity at many locations, had the worst performance. It was found that the velocity in the center of the cabin, such as positions 5, 6, and 7, was so small (< 0.1 m/s) that it was not meaningful to compare the predicted and measured results.

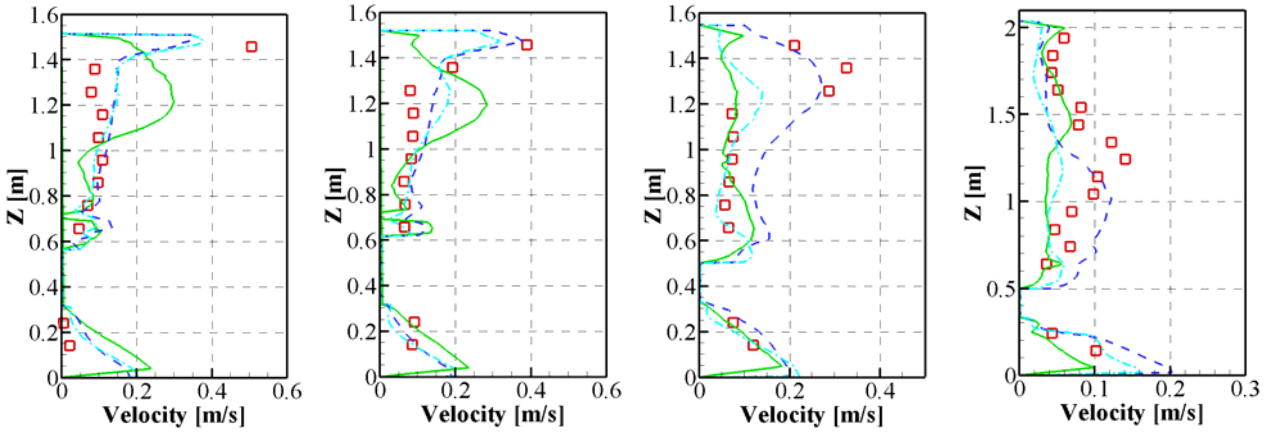

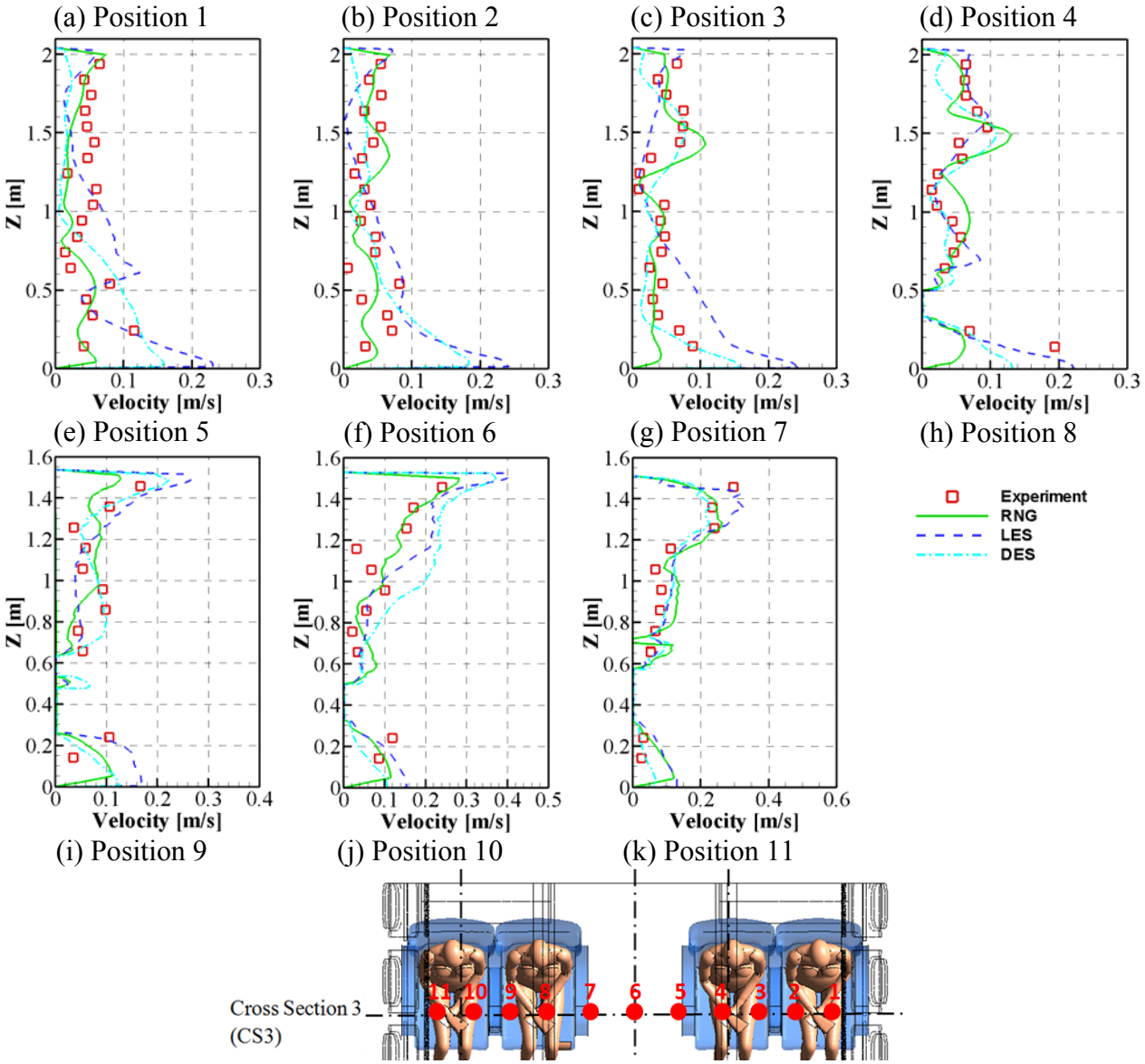

Figure 10. Comparison of the vertical velocity profiles computed and measured in cross section 3 in the fully-occupied cabin

Considering the differences between the predicted results and measured data for both conditions, the numerical simulations also have errors and inaccuracies. Since the complex geometry made it hard to generate a high quality mesh, the calculation with a second-order scheme would diverge. The first-order scheme was not sufficiently accurate. In addition, the inlet air velocity differed from one slot to another. All of these factors made the simulations very difficult to produce accurate results.

3.3 Temperature field in the fully-occupied cabin

Our experimental measurements in the unoccupied cabin were conducted for isothermal conditions as there were no heat sources in the cabin. With the heated manikins, Figure 11 shows the measured temperature field in sections CS3 and ASLS for the fully-occupied cabin. The

temperature around the manikins was a little bit higher than the air due to the heat from the manikins. Since the temperature of the floor was relatively low, the temperature field in this cabin was stratified and the vertical temperature difference between the head and ankle level was as large as 4~5 K.

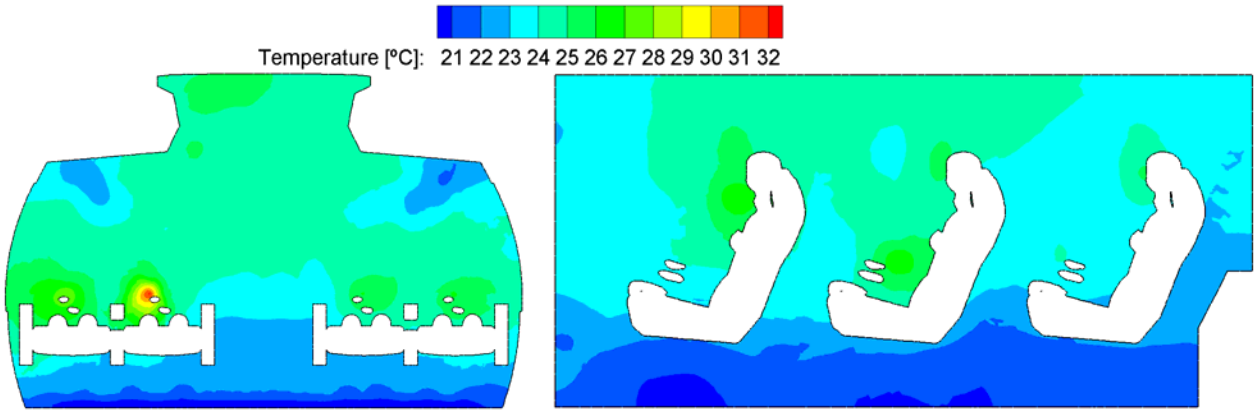

(a) Section CS3 (b) Section ASLS

Figure 11. The measured temperature distributions for the fully-occupied cabin: (a) at section CS3 and (b) at section ASLS.

This study further compares the temperature profiles at the 11 positions at section CS3 in Figure 12. It is obvious that all the turbulence models over-predicted the temperature at positions 5, 6, and 7 that were at the center of the cabin and the region close to the floor. The discrepancies might have been caused by the variation of the thermal boundary conditions and inlet air temperature. Since the measurements of the temperature field took about at least one hour, the minor change of the ambient environment could influence the temperature of the cabin wall. At other positions, the LES performed the best. The RNG k-ε model and DES still gave acceptable accuracy in predicting the air temperature.

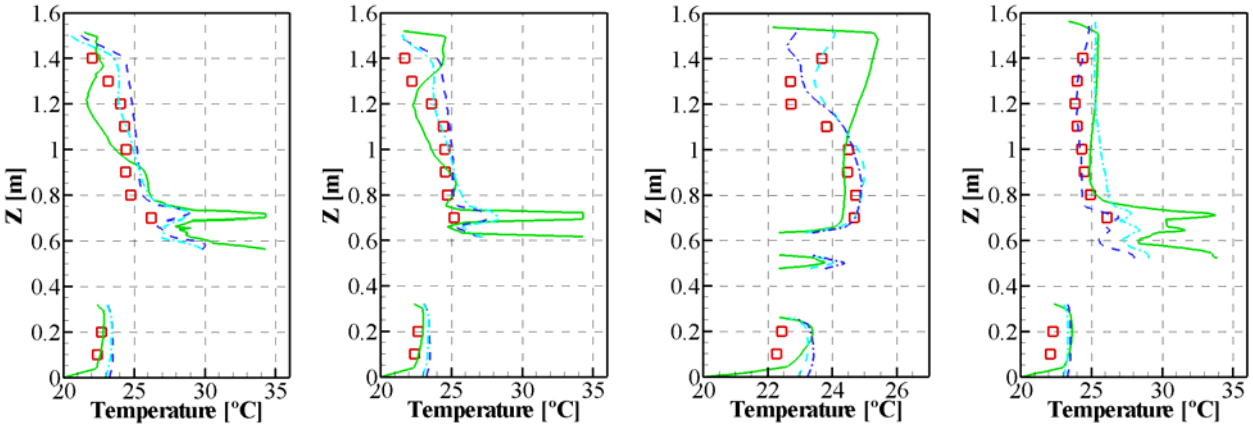

(a) Position 1 (b) Position 2 (c) Position 3 (d) Position 4

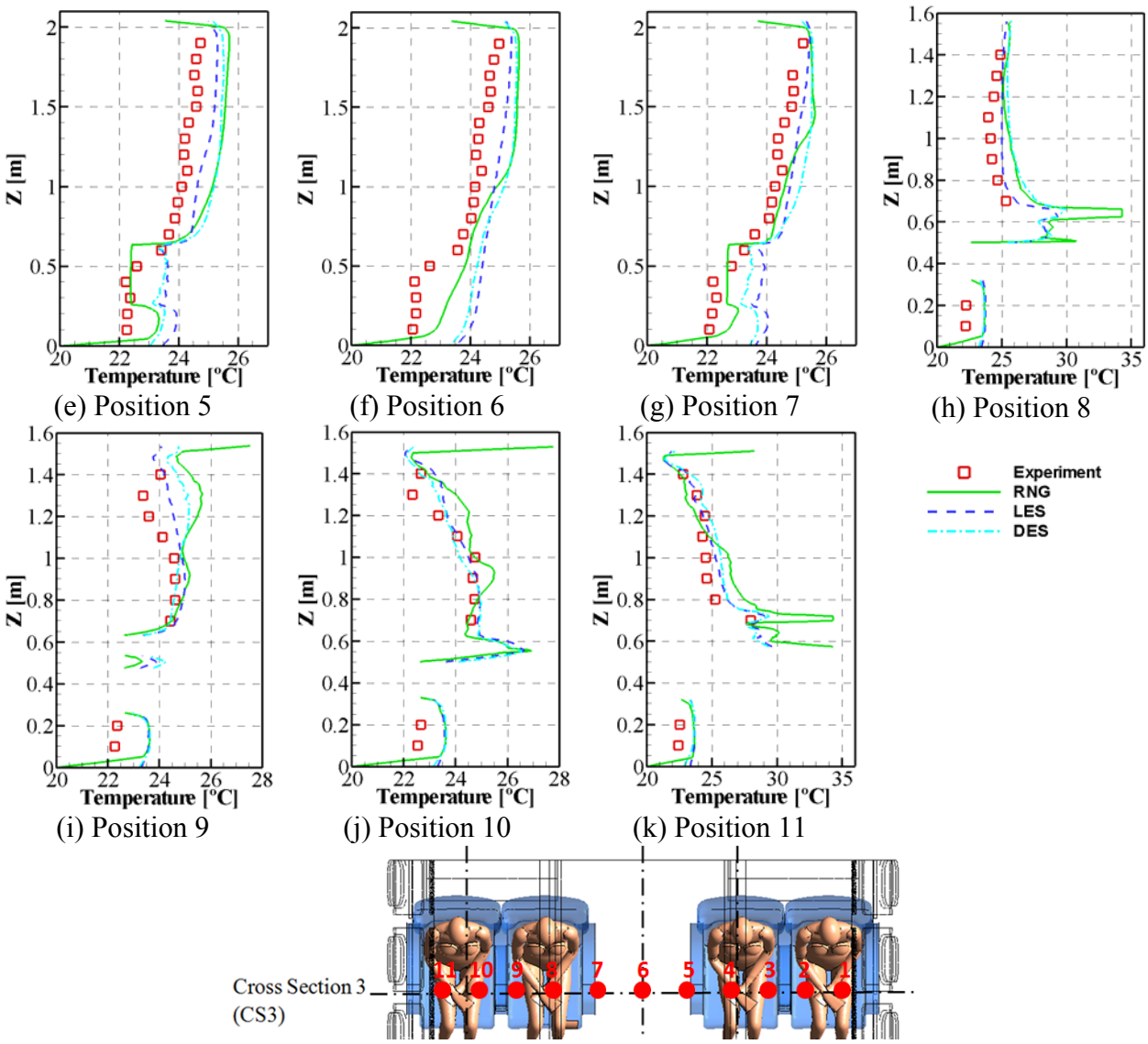

Figure 12. Comparison of the vertical temperature profiles computed and measured in cross section 3 for the fully-occupied cabin

4. Discussion

This study calculated the convective heat of the manikin in the fully-occupied cabin by the three different turbulence models. Table 3 shows that the results obtained by the models were very close, and 75% ~ 80% of the total heat (75W) was dissipated by convection. The percentile looks higher than that in buildings. A possible reason is due to the high air change rate in airliner cabins that enhanced the convection.

Table 3 Calculated convective heat flux of the manikin by three different turbulence models

Convective heat flux of manikin (W per manikin)			
Model	RNG k-ε model	DES	LES
Convective heat	56.0 W	60.2 W	58.6 W

Percentage	75%	80%	78%

Figures 13(a) and 13(c), respectively, show the turbulent kinetic energy (TKE) in section CS3 in the cabin. The TKE near the diffusers was quite high, but decayed along the airflow path and in the recirculation zones. Obstacles in the cabin, such as armrests, would increase the local turbulence. Although the TKE in the recirculation zones was low, the turbulence intensity (TI) was high, as shown in Figures 13(b) and 13(d), respectively, because of the low air velocity in these zones. Even though the flow fields for the two occupation conditions were rather different, the distributions of TKE and TI were quite similar. This may imply that the thermal plumes from the heated manikins had little influence on the turbulence.

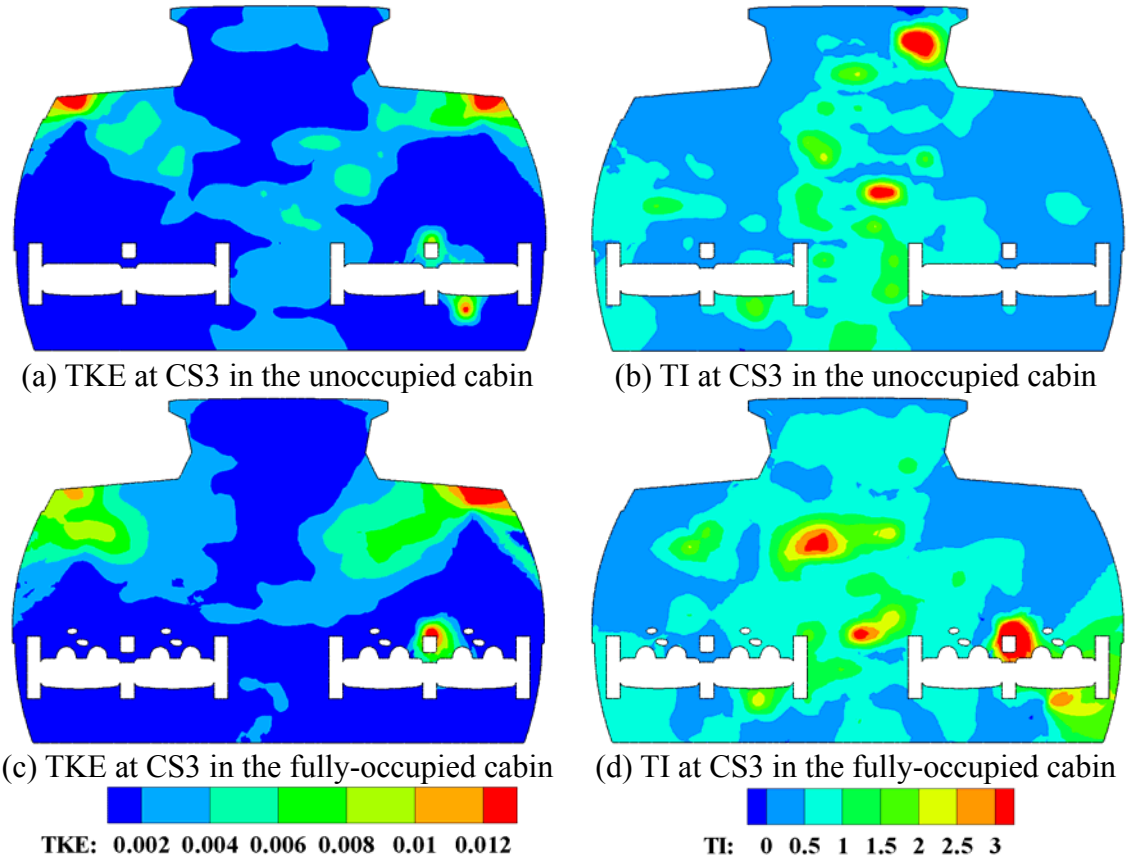

Figure 13. Distributions of turbulent kinetic energy (TKE) and turbulent intensity (TI) at section CS3 (a) and (b) in the unoccupied cabin and (c) and (d) in the fully-occupied cabin

Our previous study [25] mentioned that a laser tracking system and inverse engineering were applied to generate the digital model of the MD-82 aircraft cabin. Since the measurement accuracy was in the order of micro meters, the model obtained had a lot details. We could see clearly the patterns of fabric on the seats in the model. Figure 14(a) shows the original seat model with supporting structure beneath the seats. Those details would have negligible impact on our studies, so our study here used a simplified version as shown in Figure 14(b). To further reduce the grid number, this study also deleted the aisles on the two ends of the first-class cabin as shown in Figure 15. Since there were no heat or momentum sources in the region, this simplification may have had little influence on the flow field. To confirm the assumption, Figure

16 compares the velocity profiles at three positions at section CS3 in the cabin with and without the two extended aisles. The velocity profiles were almost the same, so the cutoff of the aisles indeed had little influence on the computed results.

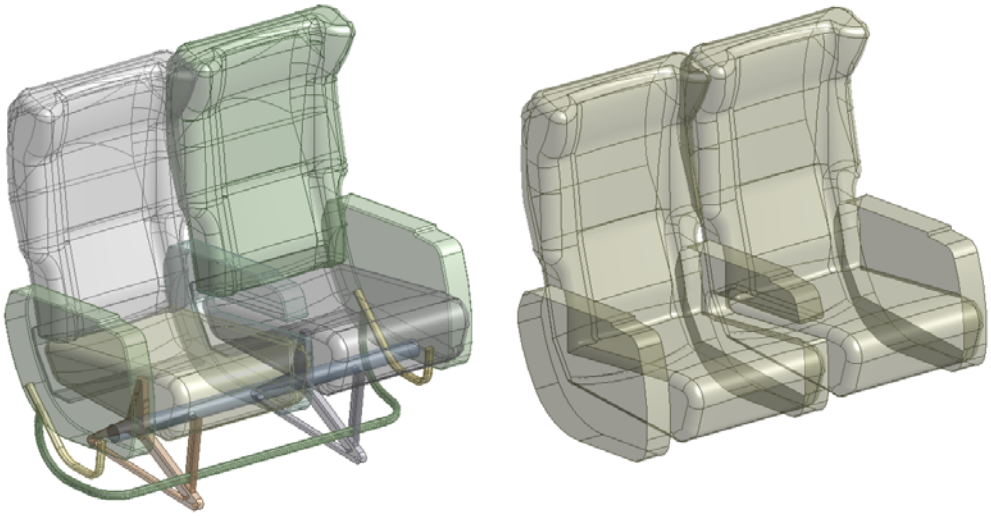

(a) Original model (b) Simplified model

Figure 14. Geometric model of the seats

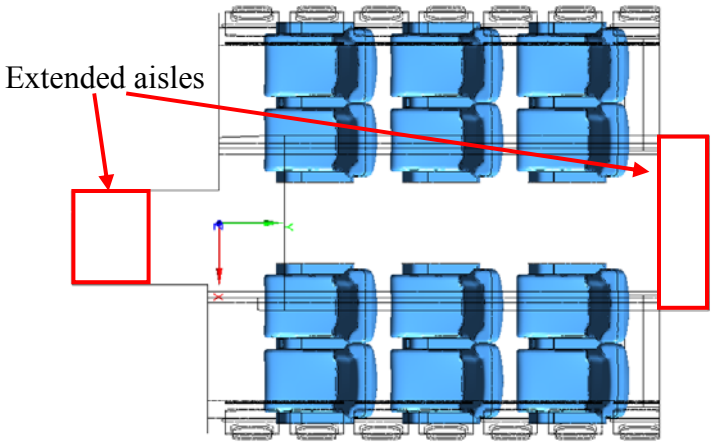

Figure 15. Geometric model with the aisles (region framed by red lines)

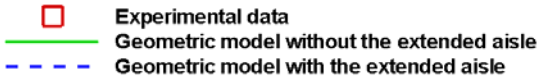

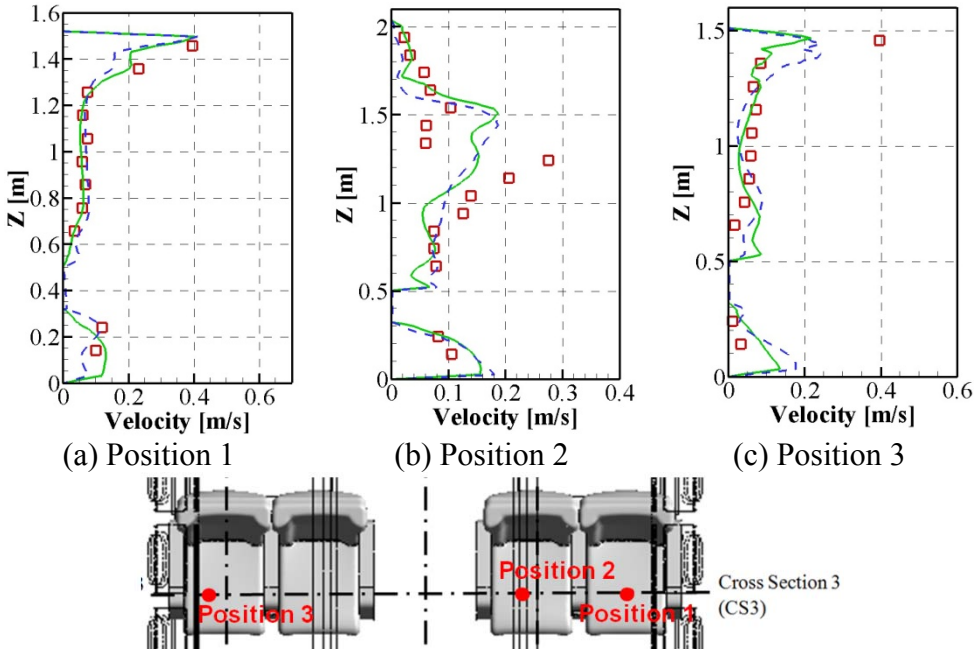

Figure 16. Comparison of the vertical velocity profiles at cross section 3 in the unoccupied cabin with and without the extended aisles.

This investigation selected one most popular model from each category of turbulence modeling methods and applied them to such a complicated flow with complex geometry. Our effort was not to prove if the models are right or wrong, but to see if those models can still produce acceptable results for engineering applications. For example, the LES and DES simulations need one magnitude order more computing time than the RNG k-ε model. The improvements on accuracy by the LES and DES may not be very evident. Then an engineer would have to think if it is worth to perform LES or DES simulations with a 100-node cluster for a week. Application engineers on airflow simulations for complex flows are very familiar with the turbulence models used. Thus, this study will provide them a good sense on the model performance and computing costs.

This study did not test or propose new turbulence models. To test a new model using such a complicated flow with the complex geometry, the results would be inconclusive. Typically one can propose or test a new model by using flow with very accurate data such as those used in reference [27]. A few good models identified in that study [27] should perform better than the most popular models used in this study, because the basic flow features in the airliner cabin are the same as those used to test the models in reference [27]. The applications of those good models are strongly encouraged for future applications, but it is beyond the aim of this investigation.

Since this study used a very complicated flow with very complex geometry, we were unable to obtain some results that would be normally obtained in simple geometry. For example, conventional wisdom is that when the grid becomes sufficiently fine, the numeric results would not change at least for RANS models. With the complex geometry, we could not really make the grid very fine due to computer capacity although the computer used was not a small one. With our finest grid, the corresponding results were not the most accurate when compared with the experimental data as shown in Figure 3. This implies that the experimental data may not be accurate or the finer grid could bring some other uncertainties. On one hand, our previous paper

[25] discussed the errors associated with the experimental data. It is extremely difficult to obtain accurate data although a half dozen of researchers worked for three years and two million dollar was spent in equipment for this experiment.

To guarantee the accuracy of the CFD simulation, it requires high-quality mesh, perfect grid-independence test, and application of high order (accuracy) scheme. In lab environment, the geometry and boundary conditions could be simple. It is possible to generate high-quality mesh with acceptable mesh size and conduct good grid-independence test. That is why researchers normally use well designed experiment with simple geometry to validate turbulence models. It is unrealistic to use a real aircraft cabin for accurately turbulence model validation and it is impossible to guarantee the accuracy of the simulations. This paper shows the reality in engineering practice and research in lab environment, which is very important for both engineers and researchers.

As mentioned in section 2.2.2, this study used the same mesh distribution for all the three turbulence models for simplicity. Actually, the LES normally requires finer near-wall mesh than the RANS modeling. Such an approach may not be appropriate and may cause some errors.

5. Conclusion

This investigation compared the performance of three turbulence models in different categories for predicting airflow and temperature distributions in the first-class cabin of a functional MD-82 aircraft. The computed results were compared with the corresponding experimental data obtained from our previous study in an unoccupied cabin [25]. Additional measurements were conducted in a first-class cabin with heated manikins on all the seats. This investigation led to the following conclusions.

For the isothermal flow in the unoccupied cabin, the LES and DES could provide better predictions than the RNG k-ε model. However, the flow results by the RNG k-ε model were also acceptable. Since the LES and DES used at least 20 times more computing time than the RNG k-ε model, the RNG k-ε model is preferred.

For the mixed convection in the fully-occupied cabin, the warm thermal plumes from the heated manikins and the cool jets from the diffusers counteracted in the cabin center. The jet momentum diminished rapidly in the cabin and the flow field was rather complex. The LES had the best performance in predicting the flow, compared with the corresponding experimental data of flow and temperature fields, although the DES results were acceptable. The RNG k-ε model failed to accurately predict the velocity distribution in some regions.

By comparing the distributions of turbulent kinetic energy and turbulence intensity measured in the unoccupied cabin with those in the fully-occupied cabin, it was found that the thermal plumes from the heated manikins had little influence on the turbulence.

Acknowledgement

The research presented in this paper was supported financially by the National Basic Research Program of China (The 973 Program) through Grant No. 2012CB720100. The authors would like to thank Chen Shen and Jiangyue Chao from Tianjin University for their help in the experiment and in the digital model of the manikins.

References

[1] National Research Council. The airliner cabin environment and the health of passengers and crew. Washington, DC, National Academy Press; 2002.

[2] Nielsen PV. Flow in air-conditioned rooms. Ph.D. Thesis, Technical University of Denmark, Copenhagen, Denmark; 1974.

[3] Chen Q. Ventilation performance prediction for buildings: A method overview and recent applications. Building and Environment 2009;44(4):848-858.

[4] Liu W, Mazumdar S, Zhang Z, Poussou S, Liu J, Lin CH, Chen Q. State-of-the-art methods for studying air distributions in commercial airliner cabins. Building and Environment 2012;47:5-12.

[5] Smagorinsky J. General circulation experiments with the primitive equations I: The basic experiment. Monthly Weather Review 1963;91:99-164.

[6] Deardorff J. A numerical study of three-dimensional turbulent channel flow at large Reynolds numbers. Journal of Fluid Mechanics 1970;42:453-480.

[7] Lin CH, Horstman R, Ahlers M, Sedgwick L, Dunn K, Topmiller J, Bennett J, Wirogo S. Numerical simulation of airflow and airborne pathogen transport in aircraft cabins-Part 1: Numerical simulation of the flow field. ASHRAE Transactions 2005;111(1):755-763.

[8] Yakhot V, Orszag S. Renormalization group analysis of turbulence. Journal of Scientific Computing 1986;1:3-51.

[9] Zhang Z, Chen X, Mazumdar S, Zhang T, Chen Q. Experimental and numerical investigation of airflow and contaminant transport in an airliner cabin mockup. Building and Environment 2009;44(1):85-94.

[10] Singh A, Hosni MH, Horstman RH. Numerical simulation of airflow in an aircraft cabin section. ASHRAE Transactions 2002;108(1):1005-1013.

[11] Shur M, Spalart P, Strelets M, Travin A. Detached-Eddy simulation of an airfoil at high angle of attack. Proceedings of the 4th International Symposium on Engineering Turbulence Modeling and Measurements, Ajaccio, France; 1999.

[12] Roy C, Blottner F, Payne J. Bluff-body flow simulations using hybrid RANS/LES. Proceedings of the 33rd AIAA Fluid Dynamics Conference and Exhibit, Orlando, Florida; 2003.

[13] Jouvray A, Tucker P. Computation of the flow in a ventilated room using non-linear RANS, LES and hybrid RANS/LES. International Journal for Numerical Methods in Fluids 2005;48(1):99-106.

[14] Jouvray A, Tucker P, Liu Y. On nonlinear RANS models when predicting more complex geometry room airflows. International Journal of Heat and Fluid Flow 2007;28:275-288.

[15] Rosenstiel M, Rolf-Rainer G. Segmentation and classification of streaks in a large-scale particle streak tracking system. Flow Measurement and Instrumentation 2010; 21:1-7.

[16] Sze T, Wan M, Chao C, Fang L, Melikov A. Experimental study of dispersion and deposition of expiratory aerosols in aircraft cabins and impact on infectious disease transmission. Aerosol Science and Technology 2009;43:466-485.

[17] Poussou S, Mazumdar S, Plesniak MW, Sojka P, Chen Q. Flow and contaminant transport in an airliner cabin induced by a moving body: Scale model experiments and CFD predictions. Atmospheric Environment 2010;44(24):2830-2839.

[18] Mazumdar S, Poussou S, Lin CH, Isukapalli SS, Plesniak MW, Chen Q. The impact of scaling and body movement on contaminant transport in airliner cabins. Atmospheric

Environment 2011;45(33):6019-6028.
[19] Sun Y, Zhang Y, Wang A, Topmiller J, Bennett J. Experimental characterization of airflows in aircraft cabins, part I: Experimental system and measurement procedure. ASHRAE Transactions 2005;111(2):45-52.
[20] Zhang Y, Sun Y, Wang A, Topmiller J, Bennett J. Experimental characterization of airflows in aircraft cabins, part II: Results and research recommendations. ASHRAE Transactions 2005;111(2):53-59.
[21] Wang A, Zhang Y, Sun Y, Wang X. Experimental study of ventilation effectiveness and air velocity distribution in an aircraft cabin mockup. Building and Environment 2008;43(3):337-343.
[22] Yan W, Zhang Y, Sun Y, Li D. Experimental and CFD study of unsteady airborne pollutant transport within an aircraft cabin mock-up. Building and Environment 2009;44:34-43.
[23] Bosbach J, Pennecot J, Wagner C, Raffel M, Lerche T, Repp S. Experimental and numerical simulations of turbulent ventilation in aircraft cabins. Energy 2006;31(5):694-705.
[24] Günther G, Bosbach J, Pennecot J, Wagner C, Lerche T, Gores I. Experimental and numerical simulations of idealized aircraft cabin flows. Aerospace Science and Technology 2006;10(7):563-573.
[25] Liu W, Wen J, Chao J, Yin W, Shen C, Lai D, Lin CH, Liu J, Sun H, Chen Q. Accurate and high-resolution boundary conditions and flow fields in the first-class cabin of an MD-82 commercial airliner. Atmospheric Environment 2012;56:33-44.
[26] Sorensen D, Voigt L. Modeling flow and heat transfer around a seated human body by computational fluid dynamics. Building and Environment 2003;38(6):753-762.
[27] Zhang Z, Zhang W, Zhai Z, Chen Q. Evaluation of various turbulence models in predicting airflow and turbulence in enclosed environments by CFD: part-2: Comparison with experimental data from literature. HVAC&R Research 2007;13(6):871-886.
[28] Lilly D. A proposed modification of the Germano subgrid-scale closure model. Physics of Fluids 1992;4:633-635.
[29] ANSYS Fluent 12.0 Documentation. Fluent Inc., Lebanon, NH; 2009.
[30] Wolfstein M. The velocity and temperature distribution of one-dimensional flow with turbulence augmentation and pressure gradient. International Journal of Heat and Mass Transfer 1969;12:301-318.
[31] Chen HC, Patel VC. Near-wall turbulence models for complex flows including separation. AIAA journal 1988;26(6):641-648.
[32] Kader B. Temperature and concentration profiles in fully turbulent boundary layers. International Journal of Heat and Mass Transfer 1993;24(9):1541-1544.
[33] Liu W, Lin CH, Liu J, Chen Q. Simplifying geometry of an airliner cabin for CFD simulations. Proceedings of the 12th International Conference on Indoor Air Quality and Climate, Austin, Texas, 2011.